# Photoinduced Gas-Phase Electron Transfer Reactions

**G. A. Zalesskaya,**[1,2] **E. G. Sambor,**[1] **and N. N. Bely**[1]

The electron transfer quenching process, when a reactive excited state is singlet or triplet, for gas-phase systems (benzophenone and anthraquinone with amines and pyridine as well as carbazole with halomethanes) was systematically investigated using time-resolved fluorescence. Bimolecular rate constants were obtained. Variable-temperature measurements were performed for eight donor–acceptor pairs. It was found that under solvent-free conditions various quenchers differing in photochemical reactivity led to change in quenching rates by almost three orders of magnitude. Positive and negative temperature dependences for the electron transfer rate constants were observed. The data were analyzed in terms of the Marcus–Jortner theory.

## INTRODUCTION

Mechanisms and rates of gas-phase photochemical reactions between complex molecules (carbazole, benzophenone, anthraquinone) excited by laser radiation and bath gases (electron donors—aliphatic amines: diethylamine, dibuthylamine, cyclohexylamine, triethylamine and pyridine or electron acceptors—halomethanes: $CHBr_3$, $CH_2Br_2$, $CCl_4$, $CHCl_3$) were investigated as these molecules were able to participate in important photochemical reactions such as hydrogen abstraction, electron or proton transfer. Such a kind of model systems with well-known relevant parameters can be studied by different methods and make possible to reveal many important features of photochemical reactions common with systems of biological interest.

Up to now a few studies, cited in [1], have been devoted to electron-transfer reactions of polyatomic molecules in a gas-phase where photochemical behavior of interacting molecules depends only on their individual properties and an additional contribution of surrounding solvent molecules does not exist. The aim of the present work is to study the influence of molecule properties, vibrational energy excess and temperature on intermolecular electron transfer (ET) for excited polyatomic molecules in gas-phase.

## EXPERIMENTAL

Emission of benzophenone and anthraquinone vapors appearing after excitation of ketones to the singlet state $S_1$ by nitrogen laser radiation (Lambda Physik FWHM $\cong$ 10 ns, $\lambda = 337$ nm, repetition rate of 10 Hz) consists of spectrally overlapping delayed fluorescence (DF) and hot phosphorescence with equal decay time and with primary DF contribution to total emission. The efficient $S_1 \rightsquigarrow T_1$ intersystem crossing at a rate $k_{ST} = 10^{11}$–$10^{12}$ s$^{-1}$ makes it possible to prepare vibrationally excited triplet molecules with $E_{vib} = (h\nu - E_T)$, where $h\nu$ and $E_T$ are the energies of exciting quantum and triplet level, respectively. For vibrationally excited molecules two components of DF with collisionless decay times of 10 and 200 $\mu$s for benzophenone, 2.0 and 400 $\mu$s for anthraquinone were used. Under an amine pressure of more than 3 Torr, the fast component disappears. The luminescence of carbazole vapor consists of fast and slow

components. The former is the fluorescence of vibrationally excited molecules from the $S_1$ state as under the halomethane pressure used ($P < 3$ Torr) vibrational equilibrium is absent in $S_1$ due to the short lifetime of the singlet carbazole molecules (45 ns at $T = 403$ K). The latter is caused by both triplet–triplet annihilation and thermal activation of the triplet molecules.

Samples were prepared in a heated quartz cell connected via dry valve with a vacuum system and evaluated to $10^{-6}$ Torr. The concentration and temperature of vapors required in experiments were controlled with the help of two separate furnaces. Polyatomics were sublimated and zone refined. They were stored in a side arm of the cell in excess and kept at a constant temperature which controlled a vapor pressure. The vapor temperature was kept constant with the help of an upper furnace. Temperature was measured with three calibrated thermocouples located at different positions. During the measurements the temperature was constant to $\pm 0.5°$. Liquid amines and halomethanes were purified by multiple vacuum distillations. These liquids were stored in a bulb on vacuum rack and deoxygenated by the freeze-pump-melt method. After that they were added into the cell from the vacuum system via a dry valve. The gas mixture was kept during several hours in order to insure that gas mixture was in thermal equilibrium with the cell wall.

Quenching the laser-induced time-resolved fluorescence of carbazole from the $S_1$ state and DF of benzophenone, anthraquinone by chemically active bath gases was used to identify the mechanism of photoinduced reactions and to evaluate the ET rate constants. The fluorescence decay time within a time interval up to 500 $\mu$s was measured by a system, consisted of Hamamatsu photomultiplier (R 1828-01) and a Tektronix digital oscilloscope (TDS 3032B, 300 MHz) connected to an IBM PC. Each experimental point for decay rates was obtained by averaging over 1000 signals. A dual channel signal acquisition technique was used to normalize for short to short fluctuation in the laser intensity.

To investigate the nature and efficiency of photochemical processes, the dependences of fluorescence time-integrated intensities $I$ and decay rates $k$ on a bath gas pressure were analyzed. In the presence of bath gases the emission spectra, intensities $I$ and decay rates $k$ under study varied with $P_{bg}$ in the following manner.

1. DF spectra of carbonyl compounds with amines and the fluorescence spectrum of carbazole with halomethanes do not demonstrate a change in the spectral shape; additional luminescence in the long wave part of the luminescence spectra is not
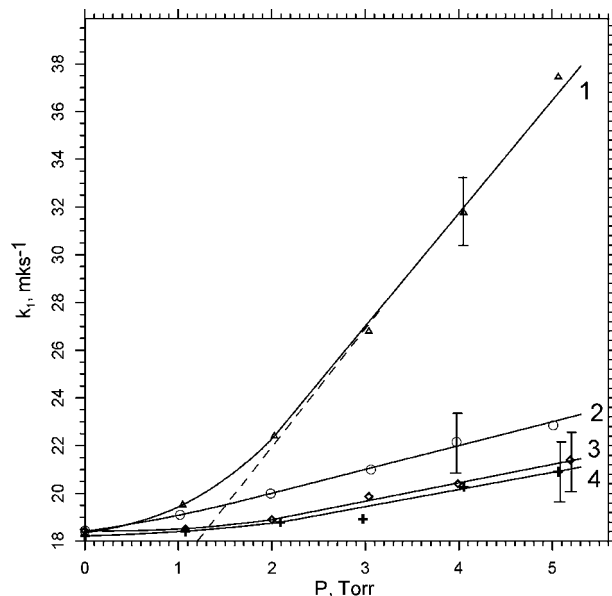


**Fig. 1.** Decay rate dependences for the fast component of carbazole fluorescence on pressure: 1—$CHBr_3$, 2—$CCl_4$, 3—$CH_2Br_2$, 4—$CHCl_3$.

found, although the emission intensities decrease strongly with a bath gas pressure growth.

2. As seen from Figs. 1–2, the decay rates $k$ increase linearly as the bath gas pressure grows:
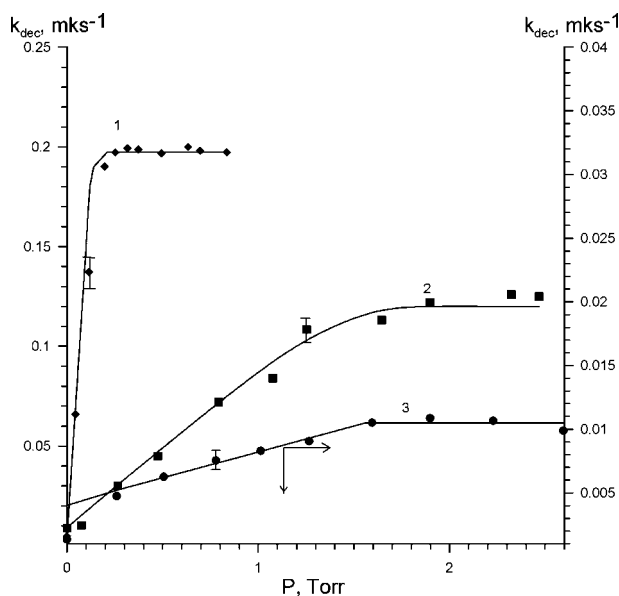
$$k = k_0 + k_q P_{bg}$$



**Fig. 2.** The rate constant dependences for the slow component of anthraquinone DF on pressure diethylamine (1), cyclohexylamine (2), pyridine (3) at $T = 433$ K.

**Table I.** Fluorescence Quenching Rate Constants $k_q$ for Excited Carbazole ($E_{ox} = 1.1$ V, $E_{S1} = 3.59$ eV, $E_{vib}$ (403 K) $= 2891$ cm$^{-1}$) with Different Halomethanes in Vapor Phase, Halomethane Reduction Potentials, $E_{red}$, Average Vibrational Energies $E_{vib}$ at $T = 403$ K, Free Energy $\Delta G_{et}$

| Halomethanes | $(-E_{red})$, V | $E_{vib}^D$, cm$^{-1}$ | Vapors $k_q(10^{-6}$ s$^{-1} \cdot$ Torr$^{-1})$ | $k_q(10^{-9}$ M$^{-1} \cdot$ s$^{-1})$ | Solutions [2] $k_q(10^{-9}$ M$^{-1} \cdot$ s$^{-1})$ | $(-\Delta G_{et})$, eV |
|---|---|---|---|---|---|---|
| CHCl$_3$ | 1.90 | 561 | $0.65 \pm 0.03$ | $16.1 \pm 0.7$ | 0.11 (acetonitrile) | 1.03 |
| CH$_2$Br$_2$ | 1.84 | 226 | $0.66 \pm 0.02$ | $16.4 \pm 0.5$ | 0.52 (acetonitrile) 0.32 (ethanol) | 1.09 |
| CCL$_4$ | 1.68 | 1087 | $1.12 \pm 0.02$ | $25.0 \pm 0.5$ | 3.47 (ethanol) | 1.25 |
| CHBr$_3$ | 1.55 | 661 | $4.60 \pm 0.10$ | $114.0 \pm 2.5$ | 13.50 (acetonitrile) | 1.38 |

where $k_q$ is the quenching rate constant, $k_0$ is the decay rate of fluorescence without a bath gas. The quenching rate constants obtained are summarized in Tables I–II. The uncertainties shown in Tables were standard deviation of the least-squares fits to the decay rate data.

3. Adding bath gases decreases fluorescence time-integrated relative intensities according to the Stern–Volmer relation: $I_0/I = 1 + \beta \tau P_{bg} Z$, where $I_0$ and $I$ are the fluorescence time-integrated intensities for the vapor and its mixtures with bath gases; $\beta$ is the quenching efficiency; $Z$ is the rate constant of gas kinetic collisions; $\tau$ is the lifetime of the polyatomic molecule fluorescence without a bath gas. For benzophenone and anthraquinone DF the intensity reduction by different amines increases in the following consequence: $I_{C_5H_5N} > I_{C_6H_{13}N} > I_{C_8H_{19}N} > I_{C_4H_{11}N}$ with efficiency close to those obtained from decay rate pressure dependences.

4. In the presence of the bath gases both the negative and positive temperature dependences for the quenching rate constants are obtained in the temperature range 433–573 K (Fig. 3).

## DISCUSSION

The experimental data obtained show that in the gas phase the interactions in donor–acceptor complexes of ketones with amines or carbazole with halomethanes essentially differ from those of these molecules with neutral bath gases. There are high quenching rate constants, strong reduction of the intensities for carbazole fluorescence and ketone DF even at small pressures, more complicated dependences of the decay rates on gas pressure and temperature. The growth of quenching rate constants and decrease of fluorescence intensities with adding bath gases considerable depends on the photochemical reactivity of interacting molecules. As the data in Tables I, II show, the efficiency of photoinduced reactions in the vapor phase vary over a wide range and is higher than in solutions.

For all pairs of the molecules under study, ET is the first stage of the photochemical reaction. For carbazole solutions in the presence of halomethanes the photoinduced one-electron transfer was proposed as the first stage of the photochemical reduction of halomethanes when the reactive excited state of carbazole was singlet [2,3]. The high efficiency and reaction rates of triplet aromatic carbonyls with various amines in liquids were attributed to charge transfer interactions [4]. The following reaction mechanism was considered as the generally accepted one.

**Table II.** Delayed Fluorescence Quenching Rate Constants $k_q$ for Triplet Molecules of Benzophenone and Antraquinone with Aliphatic Amines and Pyridine, Redox Potentials, $E_{red}$, $E_{ox}$ Average Vibrational Energies $E_{vib}$, Free Energy $\Delta G_{et}$

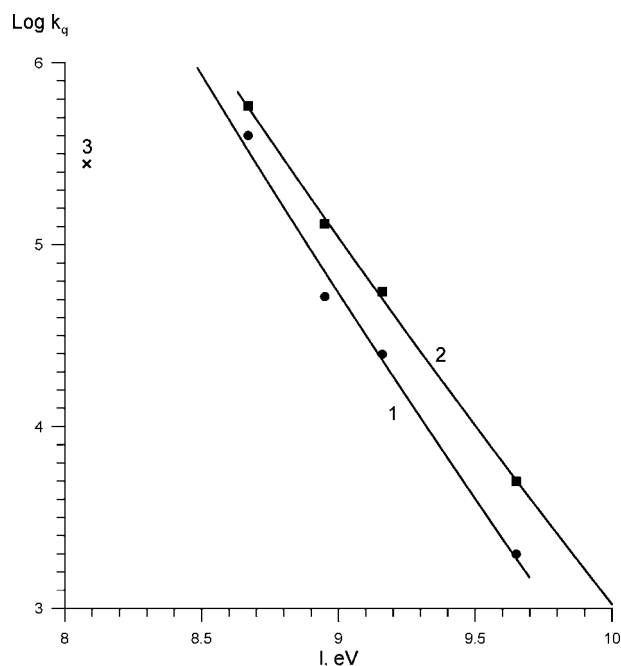| Amines | $E_{ox}$, V | $E_{vib}^D$, cm$^{-1}$ | Antraquinone $E_{vib}^A$ (433 K) $= 3816$ cm$^{-1}$, $E_{red} = -7580$ cm$^{-1}$ $k_q$, s$^{-1}$ Torr$^{-1}$ | $(-\Delta G_{et})$, cm$^{-1}$ | Benzophenone $E_{vib}^A$ (423 K) $= 4060$ cm$^{-1}$, $E_{red} = -13525$ cm$^{-1}$ $k_q$, s$^{-1}$ Torr$^{-1}$ | $-\Delta G_{et}$, cm$^{-1}$ |
|---|---|---|---|---|---|---|
| C$_5$H$_5$N | 1.84 | 1073 | $5.21 \pm 0.18 \cdot 10^3$ | 2260 | $2.00 \pm 0.10 \cdot 10^3$ | $-1310$ |
| C$_6$H$_{13}$N | 1.4 | 2013 | $7.75 \pm 0.08 \cdot 10^4$ | 4730 | $3.20 \pm 0.30 \cdot 10^4$ | 740 |
| C$_8$H$_{19}$N | 1.31 | 2848 | $1.20 \pm 0.11 \cdot 10^5$ | 6780 | $2.20 \pm 0.10 \cdot 10^4$ | 1030 |
| C$_4$H$_{11}$N | 1.01 | 1248 | $0.93 \pm 0.02 \cdot 10^6$ | 8670 | $4.30 \pm 0.15 \cdot 10^5$ | 4690 |
| C$_6$H$_{15}$N | 0.66 | 2760 | | | $2.80 \pm 0.15 \cdot 10^5$ | 6250 |
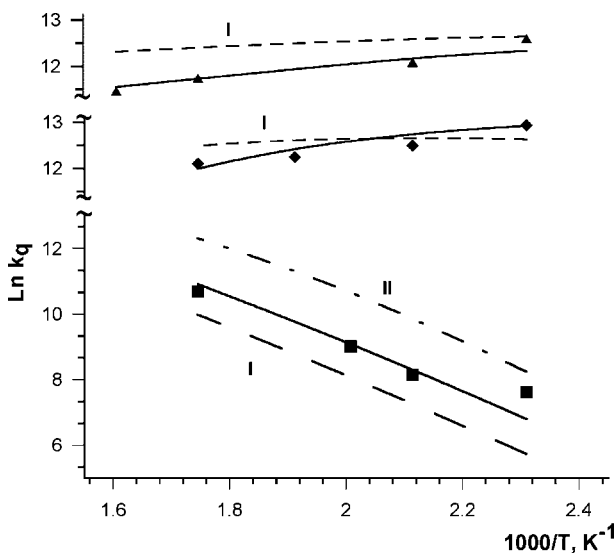
**Fig. 3.** Ln $k_q$ versus $1/T$ for benzophenone with triethylamine (2), diethylamine (&) and pyridine (∗). The solid lines correspond to Eq. (3) ($V_{DA} = 0.04\,cm^{-1}$, $\chi = 4500\,cm^{-1}$, $T = 450$ K), the dotted line (I) corresponds to Eq. (4) ($V_{DA} = 0.04\,cm^{-1}$, $\chi = 4500\,cm^{-1}$, $s_D = 0.5$, $s_A = 0.6$, $\hbar\omega_D = 1600\,cm^{-1}$, $\hbar\omega_A = 1300\,cm^{-1}$, $T = 450$ K) and the dotted line (II) corresponds to Eq. (4) ($V_{DA} = 0.05\,cm^{-1}$, $\hbar\omega_D = 1600\,cm^{-1}$, $\hbar\omega_A = 1300\,cm^{-1}$, $s_D = 0.5$, $s_A = 0.6$, $\chi = 2000\,cm^{-1}$, $T = 450$ K).



**Fig. 4.** The rate constant dependences for DF of anthraquinone (1), benzophenone (2) on donor ionization potentials. The rate constant for benzophenone DF quenching by triethylamine (3).

At the first stage, a nonbonding electron was transferred from amine to triplet carbonyl. The rapid formation of a charge transfer complex was followed either by back electron transfer and intersystem crossing from $T_1$ to a ground state $S_0$ to form ground state molecules or by proton transfer from amine to yield ketyl and amine radicals [4]. It is necessary to note that with amine pressure growth the decay rates level off. The plots of Fig. 2 at the same temperature show nonlinear quenching by amines. The back ET in a donor–acceptor complex was usually proposed to explain this kinetic behaviour in solutions [5,6], and this process can be considered as the one responsible for nonlinear quenching for gas-phase systems under study.

## Influence of the Donor Ionization Potentials on the Rate Constants of DF Quenching

The useful information can be obtained from such dependences. If charge transfer is assumed to be the primary stage of the photochemical reaction, then the ionization potential $I_p$ of the electron donor is a governing factor for acceptor luminescence quenching. For series of donors reacting with an acceptor, the linear inverse relation between $log(k_q)$ and the ionization potential of a donor molecule is often used as a criterion for the operation of the electron

transfer mechanism [7–9]:

$$\log(k_q) = \alpha I_p + \beta \qquad (1)$$

where $\alpha$ and $\beta$ are the constants for the series of donors, $k_q$ is the rate constant for the total reaction of triplets with amine. This relation was applied to the triplet state reaction of the ET for solvent-free systems. Fig. 4 demonstrates that the data for some part of amines as well as pyridine lie on a straight line. These data show that the charge transfer interaction mechanism plays an important role in the gas phase reactions for molecules under consideration. The degree of charge transfer can be estimated by the slopes of the plots. The slopes of the lines for benzophenone and anthraquinone in the gas-phase systems with amine were obtained to be $-1.9$ eV and $-2.1$ eV, respectively. The relatively low slope of $log(k_q)$ versus $I_p$ which was about ten times lower than those observed for systems with fluorescence quenching due to complete electron transfer, suggests only partial charge transfer in the photoinduced process for these molecules. It is worth noting that the degree of charge transfer in the donor–acceptor complex influences strongly the luminescence quenching features [10]. When for a certain donor–acceptor pair the free energy $\Delta G_{et}$ moves into the region of higher exothermicity and, as a consequence, the degree of charge transfer begins to differ stronger from the one obtained for other

pairs with $\Delta G_{et} > \Delta G'_{et}$. In such a case a correlation is not seen between $I_p$ of donor and decay rate of DF as for benzophenone with triethylamine in the vapor phase.

## Influence of Vibrational Excitation of the Donor and/or Acceptor Molecules on ET

The influence of photoselective excitation of a high-frequency intramolecular mode of donor and acceptor molecules on the ET process attracts considerable attention as a possible mean to control ET rates. The theoretical description of mode-specific ET was made in [1,11]. But up to now the predicted effects have no convincing experimental evidences. The experimental study of the gas-phase donor–acceptor systems can give useful information about a contribution of high-frequency modes to ET rates. Vibrationally excited donor and/or acceptor molecules in electronically excited states take place in ET for all gas-phase donor–acceptor pairs under study. Therefore there was a possibility to provide a basis for evaluating the influence of vibrational excitation on ET rates under solvent-free conditions. For this the dependences of the fast component decay rates for benzophenone and anthraquinone DF on the amine pressure were analyzed. The experimental data obtained early make it possible to conclude that the change in the decay rates and intensities of the fast component of anthraquinone and benzophenone DF are determined by intermolecular vibrational relaxation within the triplet states [12,13]. The following data analysis shows that the intermolecular reactions are insufficient within a time interval comparable to the characteristic decay time of the fast component. 1) A change in fast component decay rates for different amines is in the range of one order of magnitude (Table III). 2) The values of the rate constants are typical for intermolecular vibrational relaxation in a vibrational quasicontinuum. 3) During the characteristic decay time of the fast component, the full intensity of DF practically remains constant for the mixtures with amines, i.e. no loss of triplet molecules due to ET with amines is observed at the fast component stage. 4) The correlation between the rate constants and values of the donor half-

wave oxidation potentials $E_{ox}$ and the acceptor half-wave reduction potentials $E_{red}$ is not observed. No special features in the intensity decrease of the fast component in the presence of amines are found. So at the first stage of DF decay, the intermolecular vibrational relaxation in $T_1$ is the most effective among the other bimolecular processes. After several collisions the molecules relax from the upper vibrational level to the vibrational distribution characterized by the vibrational temperature. Initial nonequlibrium vibrational excitation of the donor molecule does not decrease or increase the ET rates under solvent-free conditions.

But for polyatomic molecules with large vibrational energy excess the distinctive feature should be taken into account for intermolecular ET between the donor and acceptor molecules. As the $E_{vib}$ estimations show, the molecules under study have $E_{vib}$ as much as 2000–4000 cm$^{-1}$. The total energy transfer involving electronic and average vibrational energy of the interacting molecules were considered in our study. For this purpose, we initially calculated the densities of the vibrational levels $N(E_i)$ and $E_{vib}$ over the total set $n$ of vibrational frequencies for considered molecules.

$$E_{vib} = \frac{\sum_{i=1}^{n} E_i N(E_i) \exp(-E_i/k_B T)}{\sum_{i=1}^{n} N(E_i) \exp(-E_i/k_B T)} \qquad (2)$$

In the heated vapors the contribution of $E_{vib}$ significantly changes the values for the free energy $\Delta G_{et}$ of the ET reaction (Tables I, II). Therefore we took into account the $E_{vib}$ values for donor and acceptor molecules in the $\Delta G_{et}$ estimations.

## Temperature Effects on ET

The temperature influences on ET have not been examined widely for gas-phase systems, although they are of great interest to reveal thermodynamic parameters of the ET process and to elucidate its mechamism. For this, both the fast and slow component decay rates as well as

**Table III.** Rate Constants $k_{rc}$ for DF Fast Component of Benzophenone and Anthraquinone with Amines at $T = 433$ K, Ionization Potentials $I_p$ for Amines, Gas Kinetic Rate Constants $Z$, Vibrational Temperature $T_{vib}$ and Collisional Efficiency $\beta = k_{rc}/Z$

| Amines | $I_p$, eV | Anthraquinone | | | | Benzophenone | | | |
|---|---|---|---|---|---|---|---|---|---|
| | | $k_{rc} \cdot 10^{-6}$, s$^{-1}$ Torr$^{-1}$ | $Z \cdot 10^{-7}$, s$^{-1}$ Torr$^{-1}$ | $T_{vib}$, K | $\beta$ | $k_{rc} \cdot 10^{-6}$, s$^{-1}$ Torr$^{-1}$ | $Z \cdot 10^{-7}$, s$^{-1}$ Torr$^{-1}$ | $T_{vib}$, K | $\beta$ |
| $C_6H_{13}N$ | 9.16 | $5.40 \pm 0.40$ | 2.9 | 600 | 0.19 | $3.1 \pm 0.3$ | 2.4 | 537 | 0.13 |
| $C_4H_{11}N$ | 8.67 | $4.16 \pm 0.30$ | 2.2 | 635 | 0.19 | $2.8 \pm 0.2$ | 1.8 | 569 | 0.16 |
| $C_8H_{19}N$ | 8.70 | $1.06 \pm 0.11$ | 2.4 | 557 | 0.04 | $3.0 \pm 0.3$ | 2.0 | 502 | 0.13 |
| $C_5H_5N$ | 9.65 | $1.00 \pm 0.10$ | 2.9 | 650 | 0.03 | $1.6 \pm 0.2$ | 2.4 | 578 | 0.07 |
| $C_6H_{15}N$ | 8.08 | | 2.8 | 570 | | $5.0 \pm 0.4$ | 2.3 | 510 | 0.22 |

the relative intensities of ketone DF and carbazole fluorescence in the presence of bath gases were measured in the temperature range 423–623 K for eight donor–acceptor pairs. The data obtained showed that for ketone vapors with different amines the positive and negative temperature dependences were observed over the same temperature range (Fig. 3) while for carbazole with $CCl_4$ and $CHCl_3$ only the negative temperature dependence was found. The activation energy $E_A$, that had been estimated from the temperature-dependent rate constants proved to be negative for benzophenone with diehtylamine ($E_A = -903$ cm$^{-1}$) and triethylamine ($E_A = -1042$ cm$^{-1}$), for anthraquinone with diehtylamine ($E_A = -713$ cm$^{-1}$) and with cyclohexylamine ($E_A = -1377$ cm$^{-1}$), for carbazole with $CCl_4$ ($E_A = -496$ cm$^{-1}$) and $CHCl_3$($E_A = -1076$ cm$^{-1}$). It may be noted that the most exothermic ET reactions gave a negative activation energy, but the others observed were positive: for example, for benzophenone with pyridine ($E_A = 3812$ cm$^{-1}$), for anthraquinone with pyridine ($E_A = 1100$ cm$^{-1}$). These data are in contrast with the original Marcus theory, which predicts the emergence of a positive activation barrier in all cases and a strong temperature dependence in the "inverted" region.

## The Dependence of the Luminescence Quenching Rate Constants on the Free Energy for ET

The experimental data obtained confirmed the important role of intermolecular electron transfer as the first stage of the considered photochemical reactions and permitted us to test the dependence of the rate constant $k_q$ on the free energy in the electron transfer process. The golden-rule transition probability is applicable to electron transfer systems and in the Condon approximation the rate constant is given as $k_{et} = (2\pi V_{DA}^2/\hbar)\cdot F$ where $V_{DA}$ is the electron transfer matrix element; $F$ is the Franck–Condon vibrational overlap term [14,15].

The rate constants $k_{et}$ for the ET process were calculated both in the classical description [14,15]

$$k_{et} = \left(2\pi V_{DA}^2/\hbar\right)\frac{1}{\sqrt{4\pi k_B T \chi_{AD}}}\exp\left(\frac{-(\Delta G_{et} + \chi_{AD})^2}{4kT\chi_{AD}}\right)$$

(3)

and in the quantum mechanical one [1,11]

$$k_{et} = \frac{2\pi V^2}{\hbar}\cdot F = \frac{2\pi V^2}{\hbar}\cdot\frac{1}{\sqrt{4\pi \chi_{AD}k_B T}}$$

$$\sum_{n^*=0}^{\infty}\sum_{m=0}^{\infty}\exp(-s_D)\exp(-s_A)\left(\frac{s_D^{n^*}}{n^*!}\right)\left(\frac{s_A^m}{m!}\right)$$

(4)

$$\times \exp\left(-\frac{(\Delta G_{et} + \chi_{AD} + m\hbar\omega_D + n^*\hbar\omega_A)^2}{4\chi_{AD}k_B T}\right)$$

where $s_D$ and $s_A$ are the electron-vibrational coupling constants and $\hbar\omega_D$ and $\hbar\omega_A$ are the vibrational frequencies of the donor and acceptor, $\Delta G_{et} = E_{ox} - (E_T + E_{vib}) - E_{red}$. The values of $E_{ox}$ [3,16–18] and $E_{red}$ [3,19] are listed in Tables I and II. In the gas phase the relevant reorganization energy $\chi_{AD} = s\cdot\hbar\omega$ is determined only through the internal change of the donor and acceptor molecules. In such a case the reorganization energy is a sum of reorganization energies of molecular vibrations upon the ET process. To calculate $k_{et}$ by Eq. (4), vibronic contributions were included for each molecule as a single averaged vibrational mode $\hbar\omega$ which was considered as an active one in the ET process.

In Fig. 5, for example, the experimental dependence of $k_{et}$ on $\Delta G_{et}$ for benzophenone—acceptor and aliphatic amines—donors is compared with predicted ones by the classical and quantum mechanical models. The $V_{AD}$ values are assumed to be constant for all reacting pairs and taken as the "best fit" for coincidence between experiment and prediction. Only one high-frequency vibration
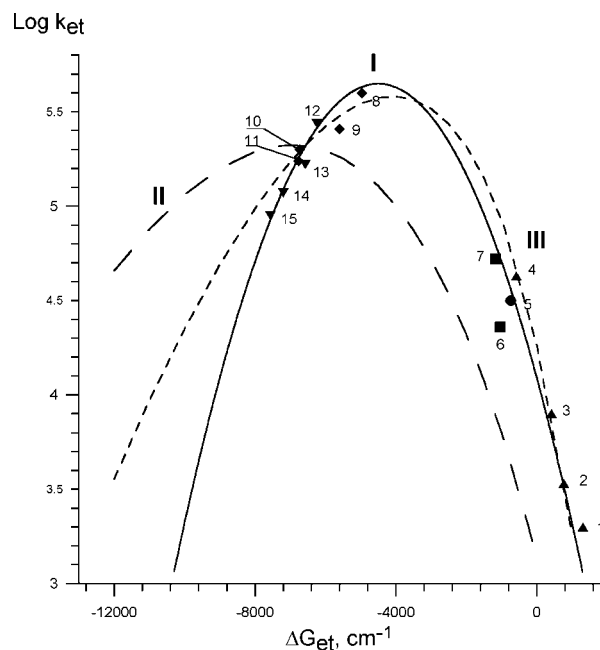


**Fig. 5.** Log $k_{et}$ versus free energy ($\Delta G_{et}$) for the ET process in a gas phase. Benzophenone acceptor; pyridine (1, 2, 3, 4 at $T = 433$, 473, 498, 573 K, respectively), cyclohexylamine (5 at $T = 433$ K), dibuthylamine (6, 7 at $T = 433$, 473 K, respectively), diethylamine (8, 9, 10, 11 at $T = 433$, 473, 523, 573 K, respectively), triethylamine (12, 13, 14, 15 at 433, 473, 573, 623 K, respectively)—donors. The solid line (I) corresponds to Eq. (3) ($V_{DA} = 0.04$ cm$^{-1}$, $\chi = 4500$ cm$^{-1}$, $T = 450$ K) and the dotted line (II) corresponds to Eq. (4) ($V_{DA} = 0.04$ cm$^{-1}$, $\chi = 4500$ cm$^{-1}$, $s_D = 0.5$, $s_A = 0.6$, $\hbar\omega_D = 1600$ cm$^{-1}$, $\hbar\omega_A = 1300$ cm$^{-1}$, $T = 450$ K), the dotted line (III) corresponds to Eq. (2) ($V_{DA} = 0.05$ cm$^{-1}$, $\hbar\omega_D = 1600$ cm$^{-1}$, $\hbar\omega_A = 1300$ cm$^{-1}$, $s_D = 0.5$, $s_A = 0.6$, $\chi = 2000$ cm$^{-1}$, $T = 450$ K).

with several populated levels was taken into account for donor and acceptor molecules. For aliphatic amines the main contribution to $\chi_{AD}$ was made by N—H bond vibration whose frequency was considered as similar for all donors. Based on the analysis of the luminescence spectra of aromatic ketones, the frequencies of the C=O vibrations were used for $\chi_{AD}$ estimations.

There is no substantial difference between two model predictions in the normal region. A systematic decrease in the rate constants with increasing exothermicity is stronger than it was predicted by Eq. (4). As $\Delta G_{et} < 0$, the parabolic dependence predicted by the Marcus theory (Eq. (3)) is in a better agreement with the experimental data. This interesting finding may be a consequence of fast intermolecular vibrational energy transfer that proves to be faster than the intermolecular ET process in the vapor phase. At vibrational equilibrium characterised by $T_{vib}$ it is unnecessary to consider the participation of high-frequency ($\hbar\omega >> kT$) vibrational modes usually treated as the quantum ones. A further vibration–translation energy transfer occurs through the low-frequency inter-molecular vibrational modes which can be treated in the classical approximation. Just the same results have been found for triplet–triplet energy transfer in the vapor phase [20]. So quenching effects for the donor–acceptor pairs considered appear to be consistent with a dependence on redox potentials (Fig. 5). The parabolic dependence $k_q(\Delta G_{et})$ can explain the observed deviation from the linear dependence $\log k_q (I_p)$ for benzophenone with triethy-lamine. This decay rate appears to be on the other wing of the Markus curve in accordance with redox potentials of a benzophenone-triethylamine pair.

This finding is confirmed by the results of the temperature measurements. Our estimations of the $E_{vib}$ temperature variations show that they cause the $\Delta G_{et}$ values to change, in some cases to an even greater degree than the internal reorganization energy. Increase or decrease in the rate constants $k_{et}$ with temperature over a temperature range under study illustrate the temperature behaviour of $\log (k_{et})$ versus $\Delta G_{et}$. The positive and negative temperature dependences of the ET rate constants are typical for the "normal" and "inverted" Marcus regions. As follows from the data in Fig. 3, the temperature dependences predicted by the Markus theory with regard of the $E_{vib}$ contribution are in a better agreement with the experimental data than the temperature dependences given by the quantum-mechanical model.

## CONCLUSIONS

1. The most important feature of the data obtained was the experimental evidence of the inverted be-

haviour in intermolecular ET for gas-phase systems. The rate constants of ET increased with exothermicity of the process in the "normal" region, passed through a maximum, and decreased in the region of large values of $-\Delta G_{et}$.

2. The significant spread in the rate constants for ET and their temperature dependences corresponded to the Marcus-type plot. It was shown that positive and negative temperature dependences of the ET rate constants were typical for the "normal" and the "inverted" Marcus regions.

3. At fast intermolecular vibrational relaxation as compared with the ET process, the total energy (electronic and average vibrational) was transferred from one molecule to another. In such a case the rate constant behaviour for ET can be explained without invoking an individual vibrational mode of donor and acceptor molecules.

4. As the data obtained showed, for gas-phase systems, where the effect of solvent reorganization energy is absent the rate constants $k_{et}$ are higher than in solutions, but lower than gas-kinetic ones.

## REFERENCES

1. M. Bixon and J. Jortner (1999). Electron transfer from isolated molecules to biomolecules. *Adv. Chem. Phys* **106**, 35–201.
2. S. M. Bonesi and R. Erra-Balsells (2001). Electronic spectroscopy of carbazole and N- and C-substituted carbazoles in homogeneous media and in solid matrix. *J. Lumin.* **93**, 51–74.
3. S. M. Bonesi and R. Erra-Balsells (2000). Outer-sphere electron transfer from carbazole to halomethanes, reduction potentials of halomethanes measured by fluorescence quenching experiments. *J. Chem. Soc., Perkin Trans.* **2**, 1583–1595.
4. J. C. Scaiano (1973/74). Intermolecular photoreactions of ketones. *J. Photochem.* **2**, 81–118.
5. M. Yamaji, Y. Aihara, T. Itoh, S. Tobita, and H. Shizuka (1994). Thermochemical profiles on hydrogen atom transfer from triplet naphtol and proton induced electron transfer from triplet methoxynaphtalene to benzophenone via triplet exiplexes studied by laser flash photolysis. *J. Phys. Chem.* **98**, 7014–7021.
6. J. O. Singh, J. D. Anunziata, and J. J. Silber (1985). *n*-π Electron donor–acceptor complexes. II. Aliphatic amines with dinitrobenzenes. *Can. J. Chem.* **63**, 903–907.
7. H. Knibbe, D. Rehm, and A. Weller (1969). Zur Thermodinamik der Bildung von EDA-Komplexen im angeregten Zustand. *Ber. Bunsen-Ges. Phys. Chem.* **73**, 839–846.
8. Y. Matsushita, Y. Yamaguchi, and J. Hikida (1996). The photochemical reaction of excited acetophenione and benzaldehyde in the gas phase. *Chem. Phys.* **213**, 413–419.
9. J. B. Guttenplan and S. G. Cohen (1972). Triplet energies, reduction potentials, and ionization potentials in carbonyl-donor partial charge–transfer interactions. *J. Am. Chem. Soc.* **94**, 4040–4042.

10. N. A. Sadovskii, M. G. Kuzmin, H. Goerner, and K. Shaffner (1998). Temperature effects on radical ion and triplet quantum yields in excited-state electron transfer reactions of 1,12-benzperylene in acetonitrile. *Chem. Phys. Lett.* **282**, 456–461.

11. J. Ulstrup and J. Jortner (1975). The effect of intramolecular quantum modes on free energy relationships for electron transfer reactions. *J. Chem. Phys.* **63**, 4358–4369.

12. G. A. Zalesskaya, D. L. Yakovlev, and E. G. Sambor (2000). Intermolecular vibrational energy transfer in mixtures of anthraquinone with foreign gases. *Opt. Spectrosk.* **88**, 705–712.

13. G. A. Zalesskaya, D. L. Yakovlev, E. G. Sambor, and D. V. Prikchodchenko (2001). Influence of short- and long-range interaction forces on the efficiency of collisional vibrational energy transfer in the vibrational quasi-continuum. *Opt. Spectrosk.* **90**, 526–533.

14. R. A. Markus (1956). On the energy of oxidation–reduction reactions involving electron transfer. I. *J. Chem. Phys.* **24**, 966–978.

15. R. A. Markus and N. Sutin (1985). Electron transfer in chemistry and biology. *Biochim. Biophy. Acta* **811**, 265–322.

16. C. K. Mann and K. K. Barnes (1970). *Electrochemical Reactions in Nonaqueous Systems*, Marcel Dekker, New York.

17. S. L. Murov *et al.* (1993). *Handbook of Photochemistry, 2nd ed.*, Marcel Dekker, New York.

18. N. L. Weinberg and H. R. Weinberg (1968). Electrochemical oxidation of organic compounds. *Chem. Rev.*, **68**, 449–523.

19. C. Hogemann and E. Vauthey (1998). Investigation of the competition between electron and energy transfer in the quenching of aromatic ketones in the triplet state using picosecond transient grating spectroscopy. *J. Phys. Chem. A*, **102**, 10051–10059.

20. G. A. Zalesskaya, V. T. Pavlova, E. G. Sambor, and N. N. Bely (2003). Energy transfer between triplet states of organic molecules in a vapour phase. *Chem. Phys. Lett.*, **373**(5–6), 448–453.